Int J Adv Manuf Technol (2016) 86:3571–3582
DOI 10.1007/s00170-016-8456-0

ORIGINAL ARTICLE

Kinetic locus design for longitudinal stretch forming of aircraft skin components

Jingwen Peng[1] · **Weidong Li**[1] · **Jinquan Han**[1] · **Min Wan**[1] · **Bao Meng**[1]

Received: 4 November 2015 / Accepted: 1 February 2016 / Published online: 16 February 2016

Abstract Longitudinal stretch forming is a vital fabricating process for the aircraft skin components with large dimensions. Loading trajectory of clamping jaws in stretch forming is significant for the qualified skin components fabrication. However, the traditional design methods based on estimation, experience, and trial-and-error are unable to manufacture skin components precisely and efficiently. A precision design method of loading trajectory for longitudinal stretch forming was developed and discussed in this paper. The sectional profile of the stretched sheet was considered to determine an optimal deformation state in the final stretching process. In view of the optimized sectional profile, the extending method of sectional curve was proposed to define the spatial locations of the clamping jaws. Furthermore, the numerical control parameters of the stretch forming press were transformed from the kinetic locus of the clamping jaws through the mechanism-solving algorithm and the computer-aided software was developed to integrate the methodology. For a fuselage skin component, the finite element (FE) simulation and experiment were conducted to verify the validity of the methodology of loading trajectory design and the algorithm of mechanism solving. The experimental and simulative results revealed that the developed methodology and algorithm are accurate and valid for the fabrication of aircraft skin components. By the examination of the formed skin part, the developed methodology thus provided relevant knowledge for loading locus design in longitudinal stretch forming.

✉ Weidong Li
space@buaa.edu.cn

[1] School of Mechanical Engineering and Automation, Beihang University, Beijing 100191, China

Keywords Aircraft skin part · Longitudinal stretch forming · Loading trajectory design · Mechanism analysis · Finite element simulation

1 Introduction

Stretch forming is a major manufacturing process for fabricating aircraft skin components. Currently, compound aircraft skins with large transverse curvature and small longitude curvature are mainly formed through longitudinal stretch forming. During the forming process, a blank sheet is clamped at two ends by clamping jaws and then stretched over a die to obtain the skin component with minimal springback. The deformation of the sheet is determined by the loading trajectories of the grippers. Therefore, the kinetic locus of the jaws is crucial for the fabrication of the aircraft skin components in the stretch forming [1].

Traditional method for loading trajectories design in stretch forming is an experience-based and trial-error process to try out the appropriate spatial motions of jaws. Many effective methodologies of loading trajectories design were investigated to fabricate the skin components qualifiedly and efficiently. Oding et al. [2, 3] studied the loading path design for the double-curvature skin stretch forming by combining the material property with theoretical analysis. Parris [4] established a 2D analytical model and an experimental model for the stretch forming, and analyzed the influences of different forming parameters on the springback behavior. Valentin et al. [5, 6] discussed the relationship between the springback and different loading control patterns including force, displacement, and strain controls. They considered that the strain control pattern is more accurate than force control. Besides, the displacement control pattern is easier to be applied in actual forming process. Zhang et al. [7] utilized the

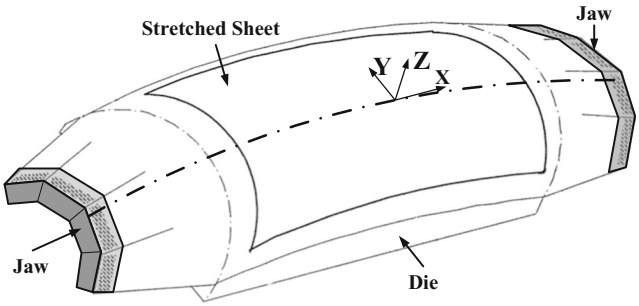

Fig. 1 Stretched sheet in longitudinal stretch forming

combination of optimization algorithm and finite element simulation to design the loading trajectory for decreasing the maximum deformation in the transverse stretch forming. He et al. [8] proposed a mathematical model to reduce the springback of a titanium-alloy skin part in cold wrap-stretch forming, and this model was verified by finite element (FE) simulation in the transverse stretch forming. By analyzing the movement of the jaw with the target shape of the profile, Liu [9] et al. optimized the post-stretching elongation through displacement loading method to reduce the forming defects of an aluminum hollow profile in stretch bending and provided an intuitive approach to design the location of the jaw. As the development of numerical control (NC) technology, the NC stretch forming press achieved the precise moving path of the clamping jaws in the stretching process. In order to realize the advantages of the precision control of the NC stretch forming press, Li et al. [10–12] presented a loading trajectories design method combining the deforming analysis in parallel planar section curve and mechanism solving of ACB series presses. The loading strategy has been applied favorably in the transverse stretch forming process. However, the parallel planar section curve cannot represent the biaxial deformation in compound-curvature skins with large transverse curvature. Therefore, the accuracy and efficiency of this parallel sectional method are not satisfied in longitudinal stretch forming. In recently years, the multi-gripper flexible stretch forming machine with forming force 2000 kN and size 1600 mm × 1200 mm was innovated and investigated to enhance the material utilization of the stretched sheet [13–15]. However, the forming capacities of the flexible stretch forming press need to be further improved to form larger skin components. Due to the complex mechanism of the longitudinal stretch forming press, the process of seeking out precision parameters was an iterative trial and error process for forming a qualified skin part. The current design method of loading trajectory was not accurate and efficient to realize longitudinal stretch forming. Therefore, a more in-depth investigation was urgently needed for the kinetic locus design in the longitudinal stretch forming.

With the development of the modern aviation industry, the fuselage skins in the new generation aircraft are becoming bigger and more complex owing to the requirements of high accuracy and integrated function [16]. The objective of this study is to achieve a quick and precise design method of loading locus for manufacturing those complicate skin components with the longitudinal stretch forming. In detail, the kinetic locus of the jaws was designed by analyzing the sectional profile of the stretched sheet. Meanwhile, a mechanism-solving algorithm was developed accordingly by transforming the loading trajectory to the control parameters of the stretch forming press. On the above-mentioned basis, the computer-aided software was developed to design the process intuitively and generate the computer numerical control (CNC) codes directly. In the end, the developed design method was verified by FE simulation and process experiment of an actual aircraft skin component.

2 Sectional analysis of the stretched sheet

In the longitudinal stretching process, the blank sheet is stretched by two jaw assemblies as shown in Fig. 1. Each jaw assembly consists of an array of adjacent sub-jaws or groups of sub-jaws to form a gripping line, which can be curved from a straight line up to an almost half-circle looking. A sectional profile of the stretched sheet and the die along the stretching direction are displayed in Fig. 2. The sheet section curve can be divided into three segments, i.e., unsupported segment (AB and CD), contact die segment (BC), and clamping segment (inside jaws).

Stretch forming is a compound deformation process including stretching and bending. In the different zones of the stretched sheet, the deforming conditions are different. The BC section is subjected to stretch-bending stress and the

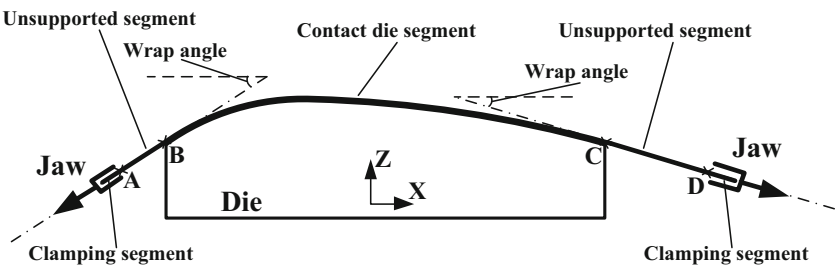

Fig. 2 Section contour in stretch forming

AB/CD sections are mainly under stretching stress. The deforming sheet shown in Fig. 2 is an ideal situation that the AB/CD segments are extended along tangent direction of the die surface at the boundary. Ordinarily, the spatial positions of the jaws shown in Fig. 3 may increase the broken risks of the sheet in stretching process and the profile error of the sheet after stretching process. As shown in Fig. 3, the ranges around B and C points undergo severe bending deformation than the case shown in Fig. 2 because of the excessive wrapping angles of unsupported segments. As analyzed by Zhang [17], the springback of a stretch-bended sheet after unloading is closely related with the bending deformation, and the excessive bending deformation aggravates the springback behavior. Therefore, the springback phenomenon in B and C areas will be worsened and the profile error in these areas of the resultant skin components will be increased. In addition, excessive wrapping angle will also increase the interfacial friction between the sheet and the die. Consequently, the risk of fracture in AB and CD segments will increase. Moreover, in the scenario shown in Fig. 3b, there is stress concentration at A and D points due to the reverse bending and the fracture will occur at these points in earlier stretching process. The comparison of the forming results in the scenario shown in Figs. 2 and 3 is presented in FE simulation verification.

Generally, the desirable state of the stretched sheet is that each longitudinal sectional profile is in accordance with the configuration as shown in Fig. 2 by the adjustment of the clamping jaws. In this scenario, the entire sheet could be in the uniform tension and precise wrapping state to decrease the broken risk and increase the profile accuracy of the skin components.

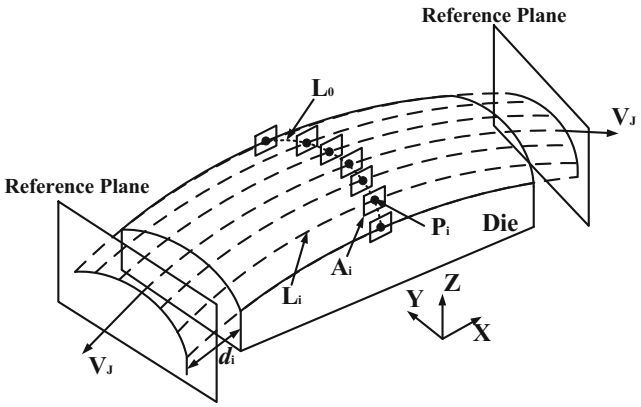

Fig. 4 Extending of section curves

3 Loading locus design and analysis

The kinetic locus of the clamping jaws is a series of spatial movement in forming process. Generally, there are four groups of movements in longitudinal stretch forming process including initial clamping, pre-stretching, jaw curving, and post-stretching. However, the appearance of the vast majority of skin components formed through longitudinally stretching is similar as shown in Fig. 1, whose sectional profiles in stretching direction is gentle and simple. As a result, the movement of the clamping jaws only requires a small wrapping angle, a short translating distance and the spatial transformation of the clamping jaws, which is not complicated in the intermediate process. Therefore, the forming result is mainly determined by the final locations of the clamping jaws in the last loading step in longitudinal stretch forming. The moving path of the clamping jaws in the intermediate process is not discussed in this study.

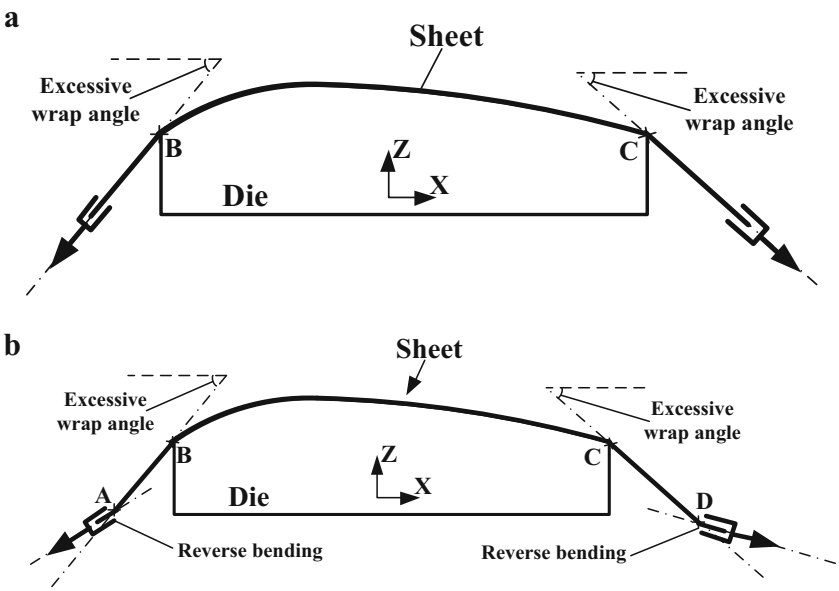

Fig. 3 Different sections with different jaw locations. **a** Section stretched by excessive wrap angle. **b** Section stretched by reverse bending at griping point

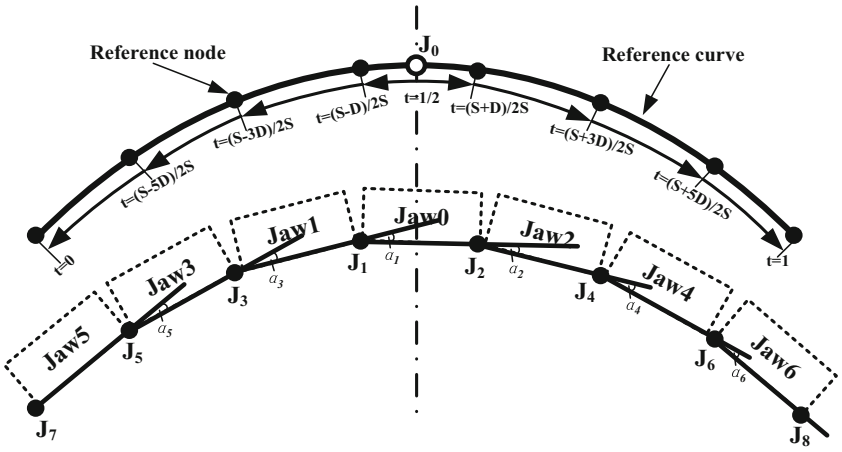

Fig. 5 Front view of the jaw curving

3.1 Kinetic locus design

The sectional analysis represents the instantaneous sectional situation for the longitudinally stretched sheet. Section curves at different positions presents the diverse profiles because of the transverse curvature of the sheet blank. To achieve an ideal section, the die surface is extended along the tangential direction at the die edge to determine the final reference planes and curves of the clamping jaws.

Considering the thickness of the sheet blank, the shape of the sheet in actual stretching process is the same as an offset surface from the die surface. As a result, the die surface is offset by a half of sheet thickness to achieve the actual configuration of the sheet blank.

Section curves that will be extended are generated by the offset surface S intersecting with a serial of planes. It is assumed that the middle range of the sheet will contact the die initially in stretching process, and this range is fixed with the die during the completely stretching process due to the interfacial friction. Therefore, the sectional planes are located on the intersection of YZ plane and surface S as shown in Fig. 4.

Detail steps of the section extending method are summarized as follows:

(1) Calculate the intersecting curve L_0 with S and YZ plane.
(2) Distribute N points evenly at L_0 as base point set $\{P_i\}$.
(3) Establish normal plane set $\{A_i\}$ of L_0 at corresponding point P_i.

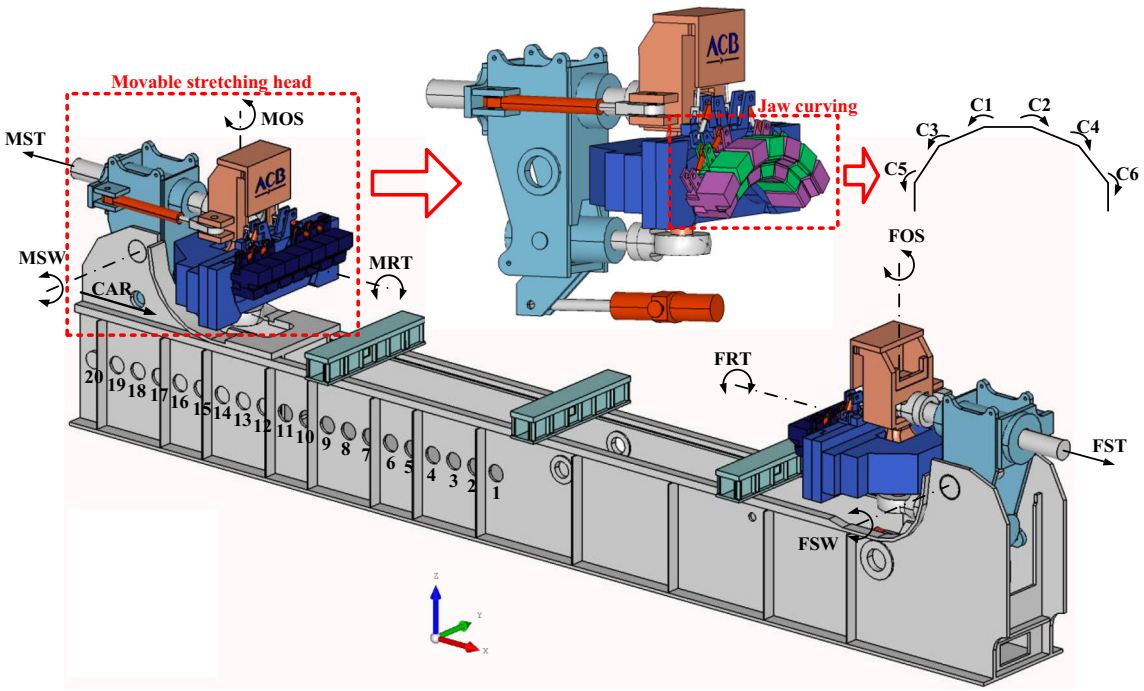

Fig. 6 ACB FEL2 × 600 stretch forming press

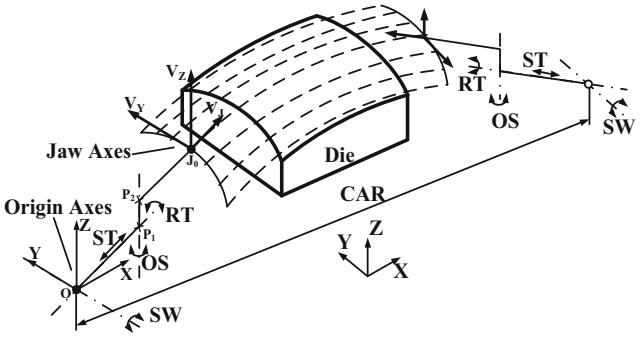

Fig. 7 Schematic illustration of FEL press mechanism

(4) Calculate intersecting curve set $\{L_i\}$ with $\{A_i\}$ and S.
(5) Extend the ends of $\{L_i\}$ along the tangential orientation by distance $\{d_i\}$.

The distance $\{d_i\}$ is calculated as follow,

$$d_i = \frac{(1+\delta)(L-L_J)-L_i}{2} \tag{1}$$

where δ is the final stretch rate, L is the sheet length, L_i is the origin length of the intersection curve, and L_J is the gripped length of blank sheet in grippers.

After the extension of the section curves, the reference plane of the jaws can be fitted by the least square method with the end point set $\{S_i(x_i,y_i,z_i)\}$ of the extended curves at one side. The reference plane function of clamping jaws is assumed as follows:

$$Ax + By + Cz + 1 = 0 \tag{2}$$

The reference curve of the jaws is fitted by the point set $\{W_i\}$ which is projected from $\{S_i\}$ to the reference plane and the fitting curve function, as presented as follows:

$$J(x,y,z) = F(t), 0 \le t \le 1 \tag{3}$$

where t is the length coefficient. Assuming the median point as a reference point (J_0) of a jaw, and t is 0.5.

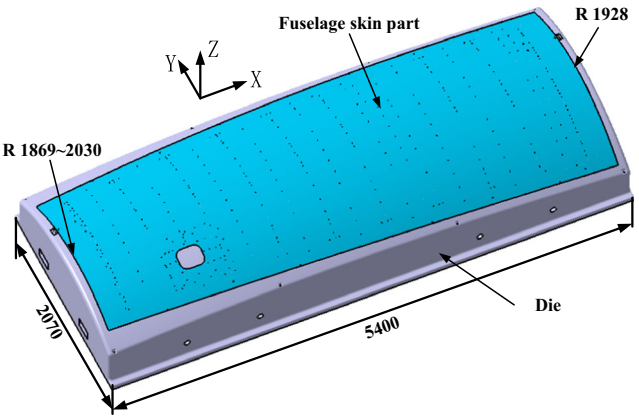

Fig. 9 Fuselage skin and die (mm)

The spatial location of a jaw can be determined by the fitted plane normal $\boldsymbol{V}_J\{A,B,C\}$ and curve $J(x,y,z)$. The jaw is curved through the rotations of the sub-jaws to accommodate the reference curve $J(x,y,z)$ as shown in Fig. 5. The rotating angle among sub-jaws can be calculated by the nodes on curve $J(x,y,z)$.

The method of computing the rotating angle of sub-jaws is a sequential searching process. The start node is the mid-point J_0 ($t_0 = 0.5$). Nodes J_1 and J_2 are searched with a half of sub-jaws' width ($D/2$) and the length coefficients are obtained as follows,

$$t_1 = t_0 - \frac{D}{2S}, \quad t_2 = t_0 + \frac{D}{2S} \tag{4}$$

Then, nodes J_3 and J_4 are searched with the width D starting from points J_1 and J_2, and the length coefficients in Eq. (5) are calculated as follows,

$$t_3 = t_0 - \frac{D}{2S} - \frac{D}{S} = t_0 - \frac{3D}{2S}, \quad t_4 = t_0 + \frac{D}{2S} + \frac{D}{S} = t_0 + \frac{3D}{2S} \tag{5}$$

The nodes J_5, J_6, J_7, and J_8 are obtained through repeating the above searching algorithm. If t is out of limits ($0 \le t \le 1$),

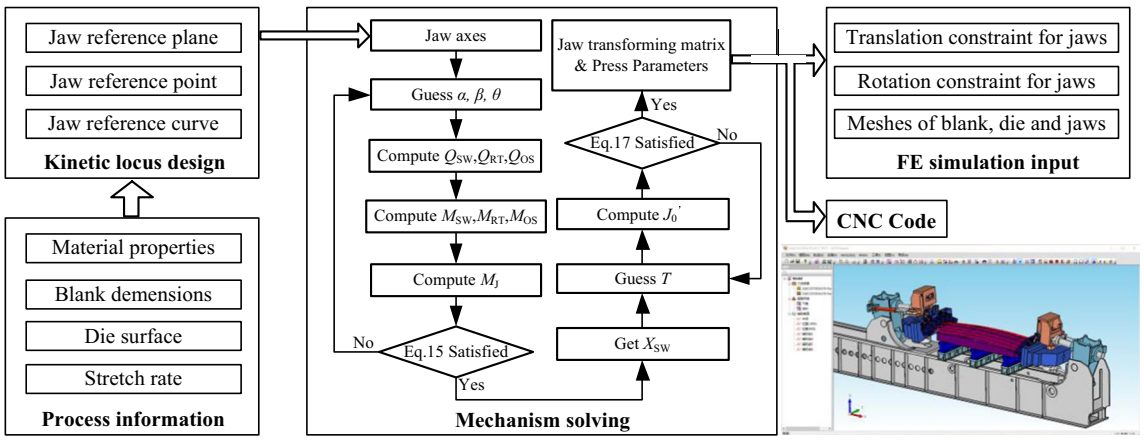

Fig. 8 Flow chart of the computer-aided software

Table 1 Control parameters of stretch press

Stretch head	SW (°)	OS (°)	RT (°)	ST (mm)
Movable	5.6	0	0	281.2
Fixed	5.9	0	0	279.7

then the searching process is terminated and the current searching nodes are the ends of jaw reference curve. Using this searching algorithm, a serial of reference nodes J on the reference curve is calculated:

$$J = \{J_7, J_5, J_3, J_1, J_2, J_4, J_6, J_8\} \tag{6}$$

The rotating angle is calculated by the reference nodes as shown in Fig. 5. For example, the rotating angle between nos. 0 and 1 sub-jaw is the angle between their reference segments J_1J_2 and J_1J_3.

3.2 Mechanism solving

In the aviation industry, the mechanical constructions of the stretching head in the different longitudinal stretch forming presses are analogous to achieve the similar motions of jaws, such as the FEL-series presses of the ACB Company and the L-series presses of the Cyril-Bath Company. The ACB FEL 2 × 600 longitudinal stretch forming press with forming force 6000 kN and size 12,000 mm × 2500 mm is employed to study the mechanism of stretch forming presses as an instance, as shown in Fig. 6. The press is mainly composed with one frame and two stretching heads. One head is fixed at an extremity of the frame and the second one is mobile and locked to the frame at a specified position depending on the format of the sheet to be formed. This press can accomplish compound movements of the jaws. There are four main available movements including stretching (ST), swinging (SW), tilting (RT), and oscillation (OS) as shown in Fig. 7. Each stretching head consists of seven sub-jaws, which can be curved (CR) by sub-jaws rotation. In stretching process, the series of press motions drive the jaws moving as the designed kinetic locus to accomplish the dragging and wrapping movements. To accomplish the digital control of the stretch forming, the mechanisms reverse solving algorithm needs to be studied to transform the kinetic locus to the motions and the control parameters of the press.

The movements of the jaws driven by the press motions can be represented by a series of transformations of the reference axes system of the jaws. The transformations of the axes system of the jaws are the functions of the control parameters of the press. The transformations of the reference axes system is started from the origin of swing axis, and the position of swing axis is determined by the location of the moveable stretching head. The location of the moveable stretching head is fixed by the lock hole in frame base and it is set up discontinuously. The lock hole position is estimated by sheet length (L) and swing angle (α). The distance of swing center (D_P) can be calculated by Eq. (7),

$$D_P = [D_0 + (n-1)W] \approx [L + 2(G-T)]\cos\alpha \tag{7}$$

where W is the distance of lock hole, n is lock hole number, D_0 is swing center distance as the stretching head is locked at the first hole, T is the extension of stretching cylinder, and G is the distance between swing center and clamping point when T is zero.

The swing angle (α) is assessed by the projecting angle between the normal of jaw plane $\boldsymbol{V}_J\{A,B,C\}$ and axis $\boldsymbol{X}$, as shown in Eq. (8),

$$\alpha_{L,R} = \tan^{-1}\frac{C_{L,R}}{|A_{L,R}|} \tag{8}$$

The average value of the swing angles of the fixed head and the movable head is an estimation to assess the lock hole in Eq. (9) as follows:

$$n \approx 1 + \left\{[L + 2(G-X)]\cos\overline{\alpha} - D_0\right\}/W \tag{9}$$

The mechanisms of the two stretching head in the ACB FEL2 × 600 press are symmetrical. As an instance, the mechanism of the moveable stretching head is studied to analyze the transformation of jaw axes system with different press motions.

The axes system of the jaw consists of J_0, $\boldsymbol{V}_J$, and the vector $\boldsymbol{V}_Y$ from J_1 to J_2 and the transformation is from the original axes system $\boldsymbol{O}$ to the axes system of the jaw in sequence as SW → RT → OS → ST. The rotating transformation is analyzed firstly.

Table 2 Sub-jaw rotation angles

Stretch head	Angles (°)					
	Nos. 5–3	Nos. 3–1	Nos. 0–1	Nos. 0–2	Nos. 2–4	Nos. 4–6
Moveable	2.0	7.0	10.0	11.0	12.0	4.0
Fixed	6.0	10.2	10.2	10.2	10.2	2.0

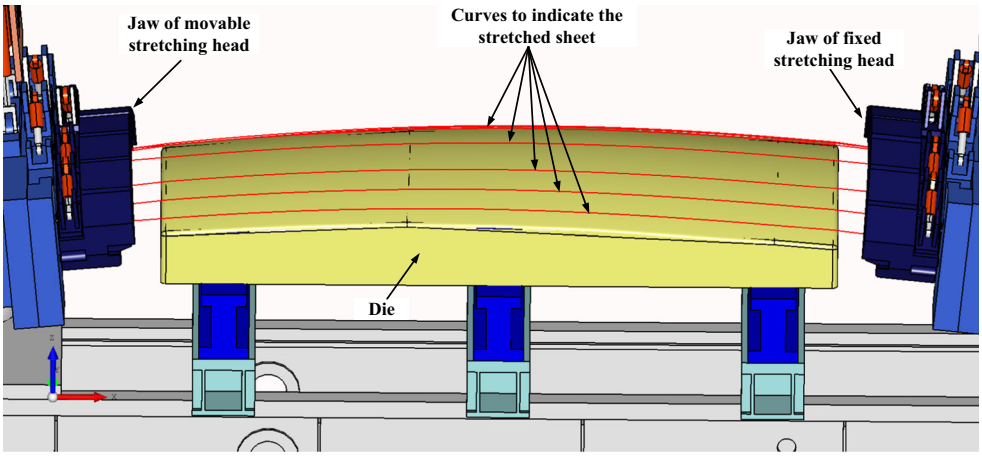

Fig. 10 Designed final locations of the jaws

The final transforming matrix of the rotations from ***O*** to the jaw axes system is expressed as Eq. (10).

$$M_J = \begin{bmatrix} x_{V_J} & x_{V_Y} & x_{V_Z} \\ y_{V_J} & y_{V_Y} & y_{V_Z} \\ z_{V_J} & z_{V_Y} & z_{V_Z} \end{bmatrix} \tag{10}$$

$\boldsymbol{M}_J$ is a matrix of composite rotating transformation multiplied by the transforming matrixes of SW, RT, and OS and the quaternions of these rotations are discussed as follows. Firstly, swinging motion is a transformation that axes system rotates around *Y*-axis by angle α and the quaternion of this transformation can be expressed as Eq. (11).

$$Q_{\mathrm{SW}} = \cos\frac{\alpha}{2} + j\sin\frac{\alpha}{2} \tag{11}$$

Secondly, tilting motion is transformation that axes system rotates around stretching axis by angle β and the quaternion of this transformation can be represented by Eq. (12).

$$Q_{\mathrm{RT}} = \cos\frac{\beta}{2} + i\cos\alpha\sin\frac{\beta}{2} - k\sin\alpha\sin\frac{\beta}{2} \tag{12}$$

Thirdly, oscillation motion is transformation that axes system rotates around the *Z*-axis after tilting by angle θ and the quaternion of this transformation can be expressed as Eq. (13).

$$Q_{OS} = \cos\frac{\theta}{2} + i\cos\beta\sin\alpha\sin\frac{\theta}{2} - j\sin\beta\sin\frac{\theta}{2} + k\cos\beta\cos\alpha\sin\frac{\theta}{2} \tag{13}$$

These quaternions correspond to the transforming matrixes $\boldsymbol{M}_{\mathrm{SW}}$, $\boldsymbol{M}_{\mathrm{RT}}$, and $\boldsymbol{M}_{\mathrm{OS}}$. Therefore, the composite transforming function is expressed as Eq. (14).

$$M_J = F(\alpha, \beta, \theta) = M_{\mathrm{OS}} \times M_{\mathrm{RT}} \times M_{\mathrm{SW}} \times O \tag{14}$$

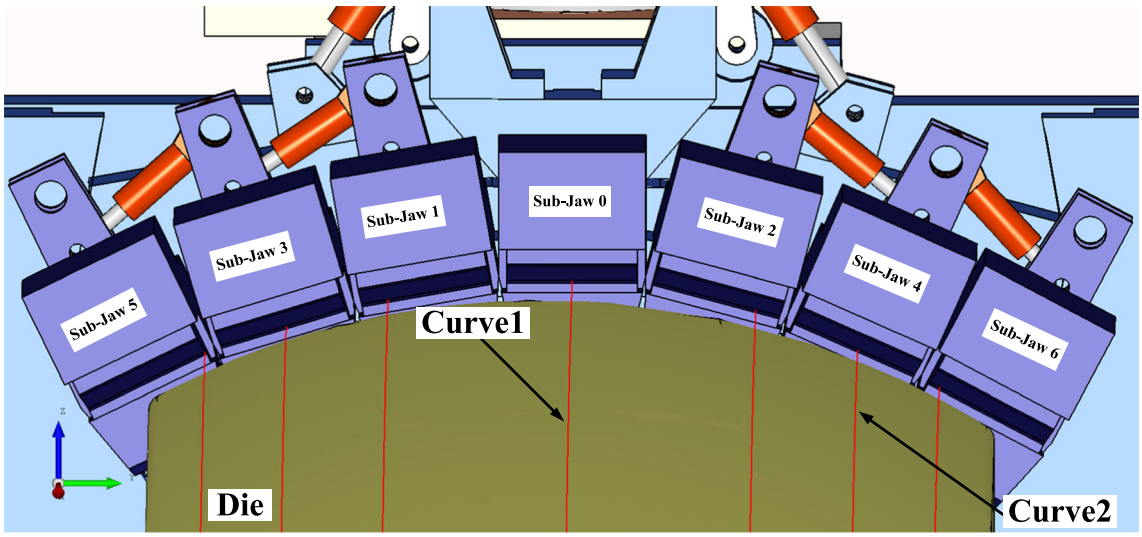

Fig. 11 Designed curving jaw of movable stretching head

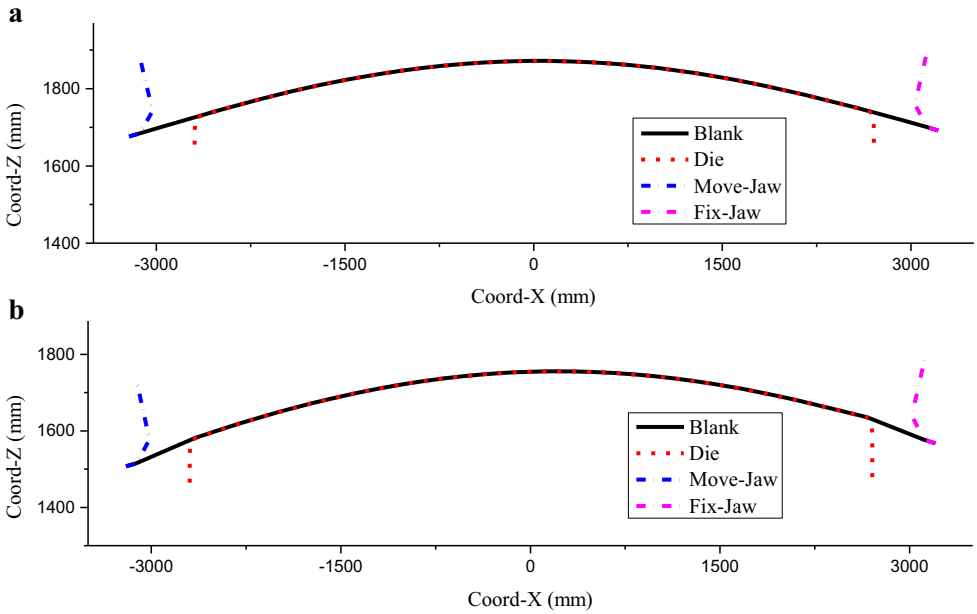

Fig. 12 Section profiles of sheet in stretch forming. **a** Curve 1. **b** Curve 2

The solving process of the FEL press mechanism is to solve the equation as follow,

$$F(\alpha, \beta, \theta) - M_J = 0 \tag{15}$$

The stretching motion is a translation along stretching direction. The swinging center reaches to an approximation point (J'_0) with J_0 after three translations ($O \rightarrow P_1 \rightarrow P_2 \rightarrow J_0$) as shown in Fig. 7. The solving equation is established with the principle that the distances of OJ_0 and OJ_0 are the same, as follows:

$$\vec{O} + (T_0 - T)\,\vec{X}_{SW} + L_2\,\vec{V}_Z + L_1\,\vec{V}_J + = \vec{J}'_0 \tag{16}$$

$$\left|\vec{OJ}'_0\right| - \left|\vec{OJ}_0\right| = 0 \tag{17}$$

where L_1 and L_2 are the length of press mechanism, T_0 is the length of the stretching axis when T is zero, and $\boldsymbol{X}_{SW}$ is the direction of stretching axis.

It is an arduous task to solve the explicit solutions of Eqs. (15) and (17) and the numerical iterative methods [18, 19] are applied to solve the approximate control parameters as long as the error is less than the accuracy of the ACB FEL2×600 press. The convergence analysis and the solution process are accomplished in the Matlab software. The algorithms of kinetic locus design and mechanism solving are all integrated in computer-aided software which is developed by authors to promote the immediacy and efficiency of longitudinal stretch forming [20]. The three-dimensionally visualizing software possesses the interface of commercial FE software and CNC code, whose solving process is shown in Fig. 8.

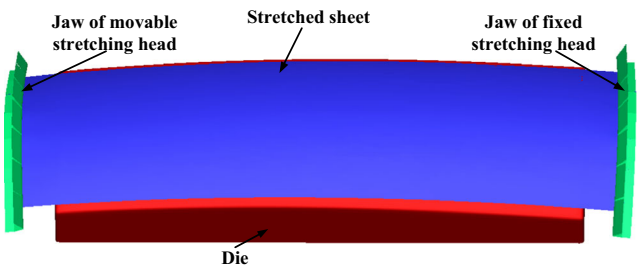

Fig. 13 The jaw and the stretched sheet in the final step of FE simulation

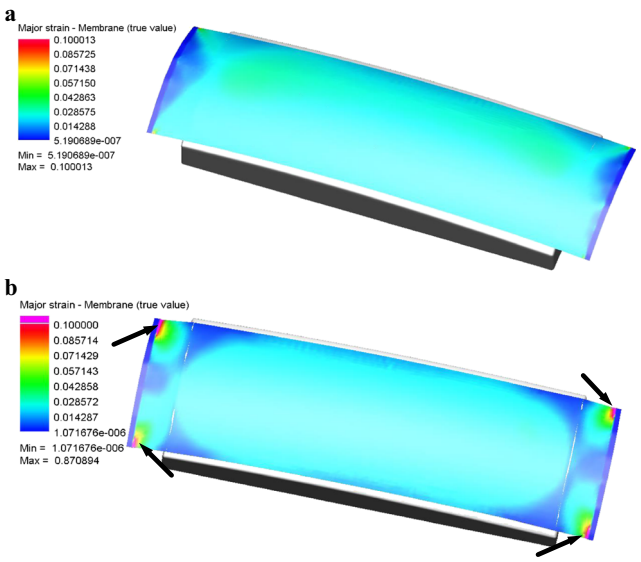

Fig. 14 Major strain distributions of the sheet. **a** Proper wrap angle, **b** Excessive wrap angle

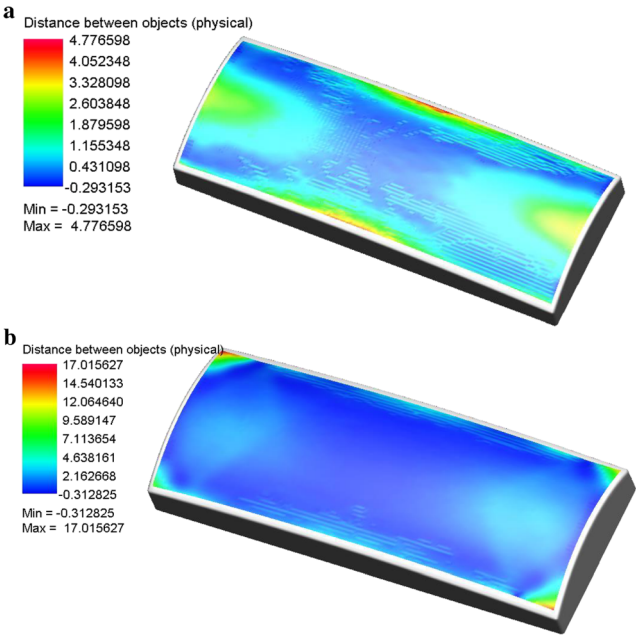

Fig. 15 Distance distributions between sheet and die after unloading. **a** Proper wrap angle. **b** Excessive wrap angle

4 Verification

The FE simulation and experiment were conducted for verification to form a fuselage skin part of a civil aircraft. A typical compound-curvature skin and die in longitudinal stretch forming are shown in Fig. 9. The transverse section at positive side of X-axis is an arc with a constant radius of 1928 mm and the radius of the transverse section at negative side varies from 1869 to 2030 mm. The profile of the skin on longitudinal section is gentle and simple. The projection of the die on X–Y plane is a rectangle with size 5400 mm × 2070 mm. The blank sheet is 2524-T3 Al alloy with the dimensions of 6300 mm × 2000 mm × 1.6 mm.

4.1 Design results

The loading trajectory in stretch forming process for verification was designed through the above-mentioned method. The control parameters of the ACB FEL2 × 600 press were computed by solving Eqs. (15) and (17) as shown in Table 1. The rotating angles of sub-jaws computed by the jaw reference nodes in Eq. (6) are shown in Table 2. The No. 10 lock hole was computed by Eq. (9) and employed in the stretch forming process.

The designed locations of the jaws at the last step of post-stretching are shown in Fig. 10. The gripping line of jaw on moveable stretching head is shown in Fig. 11. A number of curves shown in Figs. 10 and 11 were calculated by actual location of the jaws and the die to indicate the sheet configuration in practice. The coordinates of the nodes on curves 1 and 2 in Fig. 11 are exported and illustrated in Fig. 12 to show the sectional profiles. These sectional curves are in good agreement with the requirement proposed in sectional analysis and indicate that the mechanism reverse solving is accuracy on controlling wrap angle.

4.2 FE simulation

The jaws' spatial transforming matrixes in stretching process were exported to drive the meshes of jaws in FE simulation. The stretch forming process was simulated in PAM-Stamp software and the results are shown in Fig. 13. The FE simulation indicates that the stretched sheet fully covers the die without wrinkling by dragging and curving of jaws.

In FE verifying process, the designed stretching rate δ is 2.0 %. The final stretching rate of curves 1 and 2 at the pointed locations in Fig. 11 are 1.94 and 1.52 %, respectively. The stretching rate of curve 1 is closed to the designed stretching rate and the stretching rate of curve 2 is less than 2.0 % because of the swinging motion. After jaw curving, the jaw's

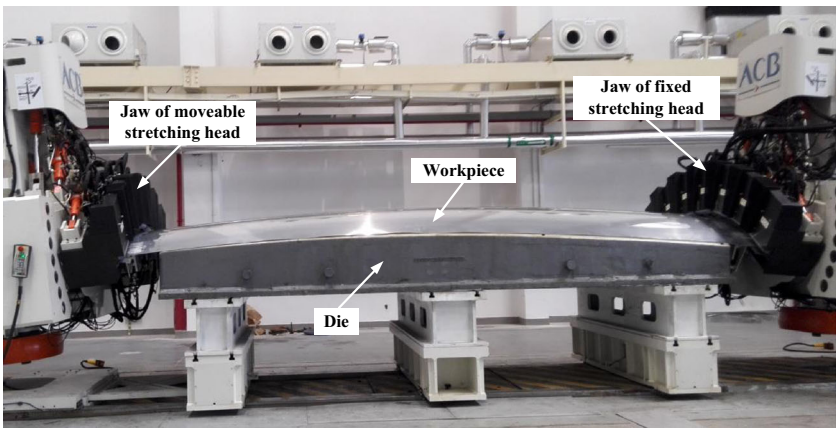

Fig. 16 Stretched sheet in loading process

plane is not parallel with *Z*-axis and the length of the sheet in the border is shorter than the length in the middle. So the strain concentration at the cross area of the blank edge and the gripper line is improved. In summary, the above-mentioned measured lengths show the good accurate control on stretching rate of the mechanism reverse solving in this study.

As described in Section 2, the excessive wrap angle will increase the risk of fracture of the unsupported segment in loading and the gap errors between the formed sheet and the die after unloading. As a comparison, another stretch process was simulated by stretching with excessive wrap angle. The simulating results of the sheet stretched with proper and excessive wrap angles are shown in Figs. 14 and 15.

The major strain distribution of the sheet in stretch process is shown in Fig. 14. The maximum strain in the sheet stretched with a proper wrap angle is 10 % within the tensile limit of this material. In comparison, the maximum strain of the sheet stretched with excessive wrap angle is larger. Moreover, the tremendous strain concentrations take place in the cross-areas of the blank edge and the gripping line, pointed by arrows in Fig. 14b, and the concentrated deformations will raise the chance of fracture in these areas.

The gap distance between the sheet and the die after unloading is shown in Fig. 15. The maximum distance of the sheet stretched with the excessive wrap angle is 17.0 mm, which is larger than the maximum distance 4.8 mm of the sheet stretched with the proper wrap angle. It is a confirmation that excessive wrap angle will increase gap errors between the formed sheet and the die.

4.3 Experiment

The stretch forming process of the fuselage skin part in Fig. 9 was accomplished by the ACB FEL 2 × 600 stretch press and the CNC codes for this stretch process were generated from the control parameters in Tables 1 and 2. As shown in Fig. 16, the configuration of the stretched sheet in experiment is the same as shown in Figs. 10 and 13. The final spatial locations of jaws designed with the method in this paper are capable of meeting the requirement of tangentially extending. The qualified part without wrinkling and fracture is shown in Fig. 17. The sheet is in total contact with the die under 5-kg pressing force and meets the common requirement of shape variation on thin skin components (thickness less than 2 mm) in aviation industry.

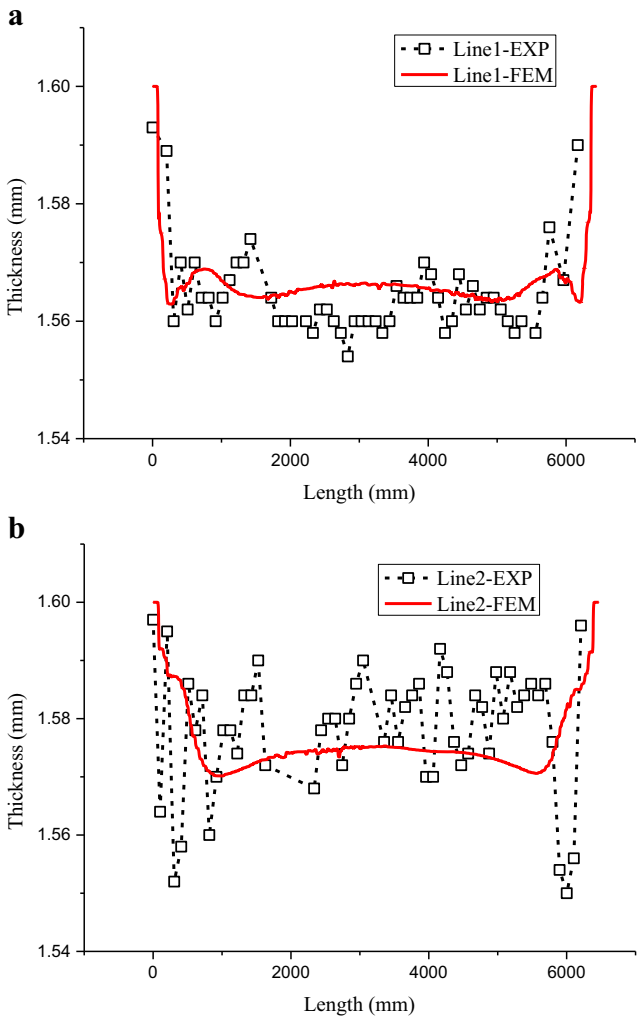

Fig. 18 Thickness distributions on the marked lines. **a** Line 1. **b** Line 2

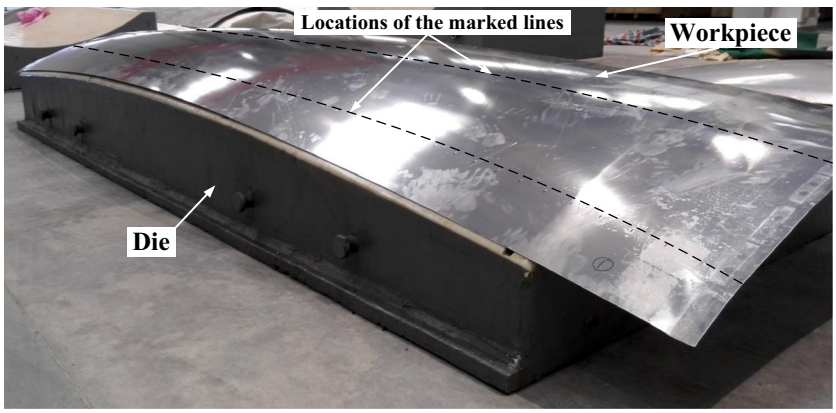

Fig. 17 Stretched sheet after unloading

The blank sheet in the experiment is marked on two parallel lines along longitudinal direction as the marks of curves 1 and 2 shown in Fig. 11. After unloading, the length of these two marked lines was measured and the values are 6415 and 6365 mm, respectively. Final stretch rates of these lines are 1.8 and 1.0 %, respectively, which indicate the same tendency as the stretch rates in FE simulation. As a result, the mechanism-solving algorithm and the CNC codes are accurate.

Thicknesses on the marked lines were measured through ultrasonic thickness gage with 100-mm space, which are shown in Fig. 18 to compared with FE simulation results. The measurement thicknesses distribute in the range of ±0.02 mm with the FE simulation values, which show the consistent trend with FE simulation results. The thickness measurement and comparison with FE simulation show the favorable prediction of the FE simulation in longitudinal stretch forming.

5 Conclusions

The kinetic locus design methodology and mechanism-solving algorithm were developed for the precision fabrication of aircraft skin components in longitudinal stretch forming. In addition, the validity and applicability of the established methodology and algorithm were verified by FE simulation and experiment. Based on the theoretical analysis and the process verification, the following conclusions are drawn:

(1) Based on the sectional analysis in longitudinal stretch forming, the unsupported segments of the sheet need to be extended along the tangent direction with the die surface to reduce the risk of fracture and the springback phenomenon, and the recommendation is proved by FE simulations.
(2) The reference plane and curve of the jaws are established by the end set of the extended section curves to determine the locations of the clamping jaws in stretch forming process. Furthermore, the designed locations of the jaws are transformed to the control parameters of the stretching press by solving the spatial transforming matrix of the jaws' axes system constructed by the reference plane and curve.
(3) The methodology of kinetic locus design and the algorithms of mechanism solving are all integrated in the computer-aided software to promote the immediacy and efficiency of longitudinal stretch forming.
(4) Based on the comparison of experiment and FE simulation in verification, the loading locus design method presented in this study facilitates the accuracy and the efficiency in fabrication of the aircraft skin components with longitudinal stretch forming.

Acknowledgments The authors would like to acknowledge the funding support to this research from the National High-Tech. R&D Program, China (no. 2006AA04Z143) and HONGDU Aviation Industry (Group) Corporation Limited.

References

1. Wisselink H, van den Boogaard A (2005) Finite element simulation of the stretch-forming of aircraft skins. In: AIP Conference Proceedings, 2005. vol A. IOP institute of physics publishing LTD, pp 60–65
2. Oding SS (1987) Controlling the formation of double curvature skin elements on a program-controlled stretch former. Izv VUZ Aviatsionnaya Tekh [Engl Trans] 30(3):47–51
3. Oding SS (1987) Control of shaping of double-curvature skins on stretch-forming equipment with programmed control. Izv VUZ Aviatsionnaya Tekh [Engl Trans] 30(4):39–43
4. Parris AN (1996) Precision stretch forming of metal for precision assembly. Massachusetts Institute of Technology, Massachusetts
5. Valentin V (1999) Implementing strain control in stretch forming. Massachusetts Institute of Technology, Massachusetts
6. Hardt DE, Norfleet WA, Valentin VM, Parris A (2001) In process control of strain in a stretch forming process. J Eng Mater Technol 123(4):496–503
7. Zhang Y, Zhou X (2006) Parameter optimization in aircraft skin stretch forming process. Acta Aeronaut Astronaut Sin 27(6): 1203–1208
8. He D, Li D, Li X, Jin C (2010) Optimization on springback reduction in cold stretch forming of titanium-alloy aircraft skin. Trans Nonferous Metals Soc China 12:2350–2357
9. Liu C-G, Zhang X-G, Wu X-T, Zheng Y (2015) Optimization of post-stretching elongation in stretch bending of aluminum hollow profile. Int J Adv Manuf Technol 1–10. doi:10.1007/s00170-015-7496-1
10. Li WD, Wan M, Zhang P, Xu CX (2004) Research on digital stretch forming system for aircraft skin. Paper presented at the 1st International Conference on new forming technology, Harbin, China, SEP. 06–09, 2004
11. Li WD, Wan M, Zhan Q, Xu CX (2004) Motion analysis and simulation control of numerical controlled transverse stretching machine for aircraft skin. J Beijing Univ Aeronaut Astronaut 30(2): 105–108
12. Li WD (2007) Technological research and system development of numerical stretch forming for aircraft skin. Beihang University, Beijing (in Chinese)
13. Li M, Han Q, Fu W, Feng P, Liu Y (2011) Study of a flexible stretch forming machine. In: Proceedings of the international conference on technology of plasticity, Aachen, Germany, 2011. pp 655–658
14. Wang Y, Li M (2014) Research on three-dimensional surface parts in multi-gripper flexible stretch forming. Int J Adv Manuf Technol 71(9–12):1701–1707. doi:10.1007/s00170-014-5610-4
15. Yang Z, Cai Z-Y, Che C-J, Li M-Z (2015) Numerical simulation research on the loading trajectory in stretch forming process based on distributed displacement loading. Int J Adv Manuf Technol 1–10. doi:10.1007/s00170-015-7470-y
16. Krammer P, Rued K, Trübenbach J (2003) Technology preparation for green aero engines. In: 2003 AIAA/ICAS international air and space symposium and exposition: the next 100 years, 2003
17. Zhang D, Cui Z, Ruan X, Li Y (2007) An analytical model for predicting springback and side wall curl of sheet after U-bending. Comput Mater Sci 38(4):707–715

18. Coleman TF, Li Y (1994) On the convergence of reflective newton methods for large-scale nonlinear minimization subject to bounds. Math Program 67(2):189–224
19. Coleman TF, Li Y (1996) An interior, trust region approach for nonlinear minimization subject to bounds. SIAM J Optim 6:418–445
20. Li W, Wan M, Jin H (2005) Computer aided engineering system for aircraft stretch forming. J Plast Eng 12:200–203 (in Chinese)